Exploring the interannual variability of extreme wave climate in the Northeast Atlantic Ocean.

Cristina Izaguirre[1], Melisa Menéndez[1], Paula Camus[1], Fernando J. Méndez [1*], Roberto Mínguez[1], Inigo J. Losada[1]

[1] Environmental Hydraulics Institute "IH Cantabria", Universidad de Cantabria, Spain
* Corresponding author

Manuscript submitted to: Special Issue on Ocean Waves. Ocean Modelling

Corresponding author address
Environmental Hydraulics Institute, IH Cantabria
c/ Isabel Torres nº15
Parque Científico y Tecnológico de Cantabria
39011 Santander
SPAIN

Phone: +34-942-201616
Fax: +34-942-266361
e-mail: mendezf@unican.es

Abstract

The extreme wave climate is of paramount importance for: i) off-shore and coastal engineering design, ii) ship design and maritime transportation, or ii) analysis of coastal processes. Identifying the synoptic patterns that produce extreme waves is necessary to understand the wave climate for a specific location. Thus, a characterization of these weather patterns may allow the study of the relationships between the magnitude and occurrence of extreme wave events and the climate system.

Eliminado: ¶

Eliminado: and

Eliminado: , and iii) its possible evolution due to changes on climate conditions

The aim of this paper is to analyze the interannual variability of extreme wave heights. For this purpose, we present a methodological framework and its application to an area over the North East (NE) Atlantic Ocean. The climatology in the NE Atlantic is analyzed using the self-organizing maps (SOMs). The application of this clustering technique to monthly mean sea level pressure fields provides continuum of synoptic categorizations compared with discrete realizations produced through most traditional methods.

Eliminado: A simple graphical representation explaining the interannual variability of extreme waves due to different synoptic patterns is then provided.

The extreme wave climate has been analyzed by means of monthly maxima of the significant wave height (SWH) in several locations over the NE Atlantic. A statistical approach based on a time-dependent generalized extreme value (GEV) distribution has been applied. The seasonal variation was characterized and, afterwards, the interannual variability was studied throughout regional pressure patterns. The anomalies of the 50-year return level estimates of SWH, due to interannual variability have been projected into the weather types of SOM. It provides a comprehensive visual representation, which relates the weather type with the positive or negative contribution to extreme waves over the selected locations.

Keywords

Eliminado: ¶

weather types, generalized extreme value distribution, climate variability, synoptic classification, Self Organizing Maps, extreme wave climate

1. INTRODUCTION

The most severe conditions of wave climate are of paramount importance on natural coastal processes (i.e. sediment transport or the development of the seaweed meadows), coastal management and engineering design (maritime works, ship design, route definition, offshore structures design, operability,…). Thus, there is a need for appropriate methods to describe these phenomena.

During the last decades, the study of the extreme wave climate has increased significantly. The statistical modelling of the extreme wave height including seasonal and interannual variability have been studied by numerous authors (Wang et al. 2001, Caires et al. 2006, Méndez et al. 2006, Menéndez et al. 2009, Izaguirre et al. 2010, Hemer, 2010). However, there is not a clear conclusion about the atmospheric situations that cause the interannual fluctuations on extreme wave heights. From this point of view, the aim of this work is to analyse the variability in the state of the atmosphere, and to investigate if these variations can explain or help to understand the complex relationships between wave forcing at a regional scale, and their effect in the interannual variability of the extreme wave climate at a local spatial scale.

Eliminado: s

Eliminado: forcings

In the earliest 70´s synoptic climatology was established as a climatological subfield with the publication of 'Synoptic climatology: methods and applications' (Barry and Perry, 1973). After that seminal work, a lot of techniques have been applied to explore and analyze the climatology in order to understand and simplify data of geophysical variables. Several statistical methods have been developed to relate synoptic-scale atmospheric circulation to local environmental responses (analysing variables like temperature, precipitation or pressure fields). The main advantage of the statistical techniques is that a large amount of complex data fields (with spatial and

Eliminado: meteorological

temporal dimensions) can be processed automatically to output a simple and readable synthesis, minimizing the human factors.

The principal component analysis (PCA) is one of the most popular techniques. PCA is especially useful to reduce the number of dimensions and identify patterns in environmental data. The data sample is projected in a space with minor dimension where the vectors of the new orthogonal base maximize the variance of the data sample. This technique removes the data dependency and data redundancy with the minimum lost of variance, which is sometimes required by the assumptions of many statistical methods.

The clustering methods try to reduce the amount of data by categorizing or grouping similar data together. These methods are used to partition the sample data into clusters defined by centroids or reference vectors representing the data in a more compact and manageable way. The self-organizing maps (SOMs) is one of the most powerful data mining techniques for clustering high-dimensional data due to its graphical visualization properties. The cluster centroids are forced with a neighborhood mechanism to a space with smaller dimension (usually a two-dimensional lattice) preserving the topology of data in the original space. Therefore, the clusters are spatially organized in the lattice of projection which gives an intuitive analysis of the information contained in the data.

Several applications of these techniques can be found in the wave climate field trying to explain relations of sea states with atmospheric patterns. Bacon and Carter (1993) showed the relationship between wave heights and the north-south atmospheric pressure in the North Atlantic (the so-called North Atlantic Oscillation, NAO). Later on, Kushnir et al. (1997) found a link between the wintertime monthly significant wave height (SWH) and monthly average sea level pressure (SLP) using a canonical

Eliminado: t
Eliminado: he
Eliminado: atio
Eliminado: of
Eliminado: since they can apply automatically.

correlation analysis. Wang and Swail (2001, 2002) applied a PCA on both the SLP and extreme wave height anomalies in the Northern Hemisphere to analyse their correlation. Woolf et al. (2002) shows that a large fraction of the wave height anomalies in the northeastern sector of the Atlantic is associated to a single pattern of pressure anomalies that resembles the NAO. Izaguirre et al. (2010) introduces the interannual variability in the generalized extreme value (GEV) distribution of extreme wave climate via the location parameter as linear covariates using principal components (PCs) of monthly sea level pressure anomalies. Le Cozannet et al. (2011) analysed the influence of teleconnection patterns in the interannual variability of the frequency of sea state modes in the Bay of Biscay, obtained from a K-means classification.

Following the hypothesis that interannual variability of the extreme wave height is induced by patterns in the atmospheric circulation, the aim of this work is to present a methodological framework to explain the relationship between extreme wave height anomalies and the synoptic situation that produces it by means of a graphical representation. To achieve this goal, a SOM analysis is carried out to process the principal components (PCs) of SLP of the NE Atlantic area, to characterize the climatology on a bidimensional lattice. The extreme wave height statistics at six different locations over the studied domain is modelled by applying a time-dependent GEV model including seasonal and interannual variability. The topology preservation property of the SOM allows defining a function on the SOM lattice corresponding to average value of extreme wave height for the reanalysis SLP dates corresponding to each of the clusters. The interannual variability of the extreme wave climate at each location projected into the climatological lattice is used to study the relationship with the synoptic states and to analyse how extreme wave probability distributions change due to changes in climatic conditions.

Eliminado: North Atlantic Oscillation (

Eliminado:)

Eliminado: en

Eliminado: e

Eliminado: the

Eliminado: reanalysis

The paper is organized as follows. Section 2 provides a description of the SLP and the wave data used. In Section 3 we present the methodology, describing the data mining techniques, PCA and SOM, and the statistical modelling of the extreme wave height. Results are shown in Section 4, the NE Atlantic weather types issued from the SOM analysis, extreme wave climate variability and the relationship between both are presented. Finally, some conclusions are given in Section 5.

2. DATA

2.1 Sea Level Pressure data

The sea level pressure fields used in this work come from the reanalysis dataset of the National Center for Environmental Prediction-National Center for Atmospheric Research (NCEP-NCAR; Kalnay et al. 1996). The SLP data consist of 6-hourly fields on a Gaussian grid with T62 resolution (about 210 km, for more details see Kalnay et al. 1996). The period of the reanalysis used in this study spans from 1948 to 2008.

The spatial domain under study spans from 25º N to 70º N and 60º W to 10º E (see figure 1) using a 5º x 5º spatial resolution grid where the SLP data are interpolated. The area is selected to capture the action center of the NAO, which is the most prominent oscillation mode in the North Atlantic. Monthly mean sea level pressure (MSLP) is extracted for the regridded spatial domain. In summary, the monthly MSLP data consist of a record of 744 monthly values from 1948 to 2008, each defined at 150 grid points.

2.2 Wave data

The wave data used in this work come from the global wave reanalysis database GOW (Reguero et al. 2012). GOW reanalysis has been generated with the third generation model WaveWatch III (Tolman 2010). The wave spectrum is computed by integration of the energy balance equation without any prior restriction about the wave spectral shape. The model is forced by 6-hourly wind fields from the atmospheric reanalysis NCEP/NCAR (with T62 Gaussian grid resolution).

This database spans from 1948 onwards with hourly resolution, and 1.5º x 1º (longitude x latitude) spatial resolution. A validation and calibration procedure was applied by using instrumental measurements from both satellite and buoy records (more details in Reguero et al. 2012, Mínguez et al. 2011, Mínguez et al. 2012).

Six locations in the east part of the North Atlantic basin are selected (see figure 1): i) a northern point (NP, lon=15ºW, lat=55ºN) around 150 km westward of Ireland, ii) a point located close to the Bretagne coast in France (BR, lon=7.5ºW, lat=49ºN), iii) a point in front of the Landes region, in the Gulf of Biscay (LA, lon=1.5ºW, lat=44ºN), iv) a point in the northwest coast of Spain, in front of Coruña (CO, lon=10.5ºW, lat=43ºN), v) a location in front of Lisbon (LI, lon=10.5ºW, lat=38ºN), and finally, vi) a point in the Azores Islands (AZ, lon=27ºW, lat=39ºN). The point of Landes is located in intermediate waters (up to 100 m) while the rest of them are in deep water.

3. METHODS

3.1 Summary of the approach

In order to establish the relationship between extreme wave height anomalies and the atmospheric forcing, we follow the next methodology:

1. Before applying any statistical technique we process the atmospheric data standardizing the MSLP fields.

2. We apply Principal Component Analysis to the standardized SLP in order to reduce dimensionality and identify dominant patterns of variability.

3. The atmospheric PCs are used for both modeling the interannual variability of extreme wave height and clustering atmospheric patterns into weather types using SOM technique.

4. For six selected locations we model the interannual variability of extreme wave height using a time-dependent generalized extreme value model. We introduce the PCs of MSLP as covariates to model interannual variability.

5. In line with the extreme wave height modeling we cluster the atmospheric PCs using the SOM technique obtaining a lattice of representative weather types of the North Atlantic.

6. Using the probability of occurrence of the SOM lattice we project the interannual variability of extreme wave height and relate weather types (atmospheric forcing) with extreme wave height anomalies.

The statistical techniques and extreme value model used are described next.

3.2 Principal Component Analysis

Eliminado: 1

The Principal Component Analysis (see Preisendorfer and Mobley, 1988) is carried out on the MSLP in order to reduce the dimensionality of the problem, preserving the maximum of the sample variance. It is a classical statistical linear compression method which gives an optimal (in a statistical sense) linear reduction of dimension (Gutierrez et al. 2004). This statistical technique is widely used in climatology to identify dominant patterns of variability and/or reduce dimensionality of climate data (Smith et al. 1996).

Con formato: Sangría: Primera línea: 1 cm

The reduction of dimensionality is achieved by creating a new set of orthogonal (hence uncorrelated) and ordered variables, the principal components, spanning the maximum variance of the data (Jolliffe 2002). Let $X(t)=[X_1(t), X_2(t),..., X_p(t)]$ be an

$n \times p$ data matrix, $\{X_i(t); i=1,\ldots,p; t=1,\ldots,n\}$ is a vector containing n (monthly) values of the i^{th} centered predictor (to avoid problems due to different scales, the variable monthly MSLP is previously standardized, related to the average over $n = 744$ instants, for each grid point, obtaining monthly MSLP anomalies), and p is the number of predictors (i.e., $p = 150$ grid points over covering the region 25ºN-70ºN, 60ºW-10ºE in the NA area). PCs components are obtained by

$$Z_i(t) = \sum_{k=1}^{p} e_{ki} X_k(t), \qquad \mathrm{i} = 1,\ldots,p; t = 1,\ldots,n \tag{1}$$

where e_m are the elements (loadings) of the m^{th} eigenvector of the covariance matrix

$$S = \frac{1}{n-1} X^T X \tag{2}$$

The analysis of the anomalies of monthly MSLP yields the spatial modes and their temporal amplitudes. The first 10 modes, explaining more than 90 % of the variability, are chosen. Note that the first two modes are correlated with the two prominent teleconnection indices of the North Atlantic: North Atlantic Oscillation (NAO) and East Atlantic (EA) pattern. The correlation between the first and second modes and the NAO Index is $r_1^{NAO} = 0.704$ and $r_2^{NAO} = 0.381$, respectively. Regarding the EA, only the correlation with the second mode is statistically significant and equal to $r_2^{EA} = 0.628$.

3.3 Time-dependent extreme model

Eliminado: monthly MSLP anomalies related to the average over n instants at the i^{th} grid point

Eliminado: p=150

Eliminado: The

Con formato: Color de fuente: Automático

Eliminado: To avoid problems due to different scales, the variable monthly MSLP is previously standardized for each grid point before applying PCA, obtaining monthly MSLP anomalies.¶

Latest advances in extreme value theory (see Coles 2001) allow a better description of the natural climate variability of extreme events of geophysical variables, specifically extreme wave height. In this work a time-dependent GEV model for monthly maxima SWH including seasonal and interannual variability is used. We have considered time-dependent location $\mu(t)$, scale $\psi(t) > 0$ and shape $\xi(t)$ parameters of the GEV (Coles 2001), with cumulative distribution function (CDF) of H_t (monthly maxima of the significant wave heights observed in month t) given by

$$F_t(H) = \begin{cases} \exp\left\{ -\left[1 + \xi(t) \left(\dfrac{H - \mu(t)}{\psi(t)} \right) \right]_+^{-1/\xi(t)} \right\} & \xi(t) \neq 0 \\ \exp\left\{ -\exp\left[-\left(\dfrac{H - \mu(t)}{\psi(t)} \right) \right] \right\} & \xi(t) = 0 \end{cases}, \qquad (3)$$

where $[a]_+ = \max[a, 0]$. The GEV distribution includes the three classical distribution families of extreme value theory: Gumbel family ($\xi = 0$); Fréchet distribution ($\xi > 0$), and Weibull family ($\xi < 0$).

Figure 2 shows the total population of SWH for each location and the monthly maxima sample. A clear seasonal variation is observed in all the points (stronger in north latitudes, North Point and Bretagne) and also a clear interannual variability can be appreciated, with severe and mild years, due to the natural climate variability. Since most of the variability is explained by seasonal behavior (Izaguirre et al. 2011) the introduction of harmonic functions to model seasonality is used (Menéndez et al., 2009). We let the model introduce the best number of harmonics in the three parameters.

Con formato: Color de fuente: Negro, Disminuido 6 pto

Con formato: Color de fuente: Negro, Disminuido 41 pto

On the other hand, the hypothesis that extreme wave climate is affected by regional SLP patterns is used. We introduce the PCs of monthly MSLP in the NE Atlantic obtained in section 3.2 as covariates to model interannual variability (Izaguirre et al., 2010). We let the model introduce up to ten PCs as linear terms in the location and scale parameter (we standardize the PCs to give all of them the same relative weight in the extreme value model).

Mathematically, the model can be expressed as:

$$\mu(t) = \beta_0 + \sum_{i=1}^{P_\mu}\left[\beta_{2i-1}\cos(i\omega t) + \beta_{2i}\sin(i\omega t)\right] + \sum_{j=1}^{10}\beta_{PCj}Z_j(t) \quad (4)$$

Con formato: Disminuido 15 pto

$$\log\left[\psi(t)\right] = \alpha_0 + \sum_{i=1}^{P_\psi}\left[\alpha_{2i-1}\cos(i\omega t) + \alpha_{2i}\sin(i\omega t)\right] + \sum_{j=1}^{10}\alpha_{PCj}Z_j(t) \quad (5)$$

Con formato: Disminuido 15 pto

$$\xi(t) = \gamma_0 + \sum_{i=1}^{P_\xi}\left[\gamma_{2i-1}\cos(i\omega t) + \gamma_{2i}\sin(i\omega t)\right] \quad (6)$$

where β_0, α_0 and γ_0 are mean values; β_i, α_i and γ_i ($i > 0$) are the amplitudes of the harmonics; $\omega = 2\pi$ year^{-1}; P_μ, P_ψ, and P_ξ determine the number of sinusoidal harmonics in a year; and *t* is given in years. The parameter β_{PCj} and α_{PCj} represents the influence on the location and scale parameters per unit of standardized Z_j in a particular month, *t*. The model selection is carried out using the pseudo-optimal method explained in Minguez et al. (2010).

Con formato: Disminuido 7 pto

The instantaneous quantile $H_q(t)$ associated with the return period $1/q$ can be obtained using:

$$H_q\left(\mu(t),\psi(t),\xi(t)\right)=\begin{cases}\mu(t)-\dfrac{\psi(t)}{\xi(t)}\left[1-\left\{-\log\left(1-q\right)\right\}^{-\xi(t)}\right] & \xi(\mathrm{t})\neq 0\\ \mu(t)-\psi(t)\log\left\{-\log\left(1-q\right)\right\} & \xi(\mathrm{t})=0\end{cases}$$

(7)

where probability q is given by $F_t(H)=1-q$. Since seasonal and interannual variability have been modeled, the quantile varies depending on the time within the year and the year itself.

The interannual variation in the time-dependent quantile can be expressed as the difference between the time-dependent quantile (H_q) and the seasonal-dependent quantile (H_{qs}), where the seasonal-dependent quantile is calculated from a regression model where only the seasonal variation is considered.

$$\delta H_q = H_q - H_{qs}$$

(8)

where δH_q is the time-dependent quantile anomaly.

3.4 Self-Organizing Maps

Interannual wave climate variability is dependent on large-scale dynamic in the atmosphere-ocean system. In this study we are interested in whether there is a direct relationship between synoptic climatology and extreme wave climate. SOM is, therefore, the selected technique to establish synoptic patterns (weather types). It is a

Con formato: Disminuido 7 pto

Con formato: Disminuido 26 pto

Con formato: Disminuido 6 pto

Con formato: Disminuido 7 pto

Con formato: Disminuido 7 pto

Con formato: Disminuido 7 pto

Con formato: Disminuido 7 pto

Eliminado: 2

statistical method developed in the field of data mining to deal with huge amounts of data efficiently. This analysis tool, from the field of artificial neural networks, supports analysis of variability in large, multivariate and/or multidimensional data sets through the creation of a spatially organized set of generalized patterns of variability from the data. A SOM summarizes the high-dimensional data space in terms of a set of reference vectors (cluster centers) having spatial organization corresponding to a two-dimensional lattice. Note that we use the PC vectors Z_i instead the original data x_i to train the SOM (Gutierrez et al. 2005) in order to eliminate noise from the signal.

The SOMs analysis provides a complementary nonlinear alternative to more frequently used but linear methods, such as PCA. SOM has several advantages, including: i) it handles nonlinear relationships, and ii) it provides a robust interpolation method in areas of the input space not present in the available training input. Another benefit, when applied to atmospheric data, is that it supports the development of synoptic climatologies with an arbitrary number of smoothly transitioning climate states, in contrast to traditional synoptic classification techniques. The projection of the results in a lattice with spatial organization makes it different to other technique, being a more powerful tool due to the easy interpretation of the results by visual inspection.

A SOM is formed by an arbitrary number of clusters (or centroids) C_k, where $k = 1...m$, (*m* is the number of clusters) located on a two-dimensional matrix for visualization purposes, that are representative of the probability density function of the input data. Each cluster C_k is associated with two vectors . First, the vector $c_k = (i_k, j_k)$ describes the position of cluster C_k on the matrix. Besides, each of the clusters C_k is associated with a reference vector $v_k = (v_{k1},...,v_{kn})$ in the space of data, where *n* is the number of month, previously defined in section 3.2. The number of selected clusters

Con formato: Disminuido 6 pto

Eliminado: the

Eliminado: reference vectors

Con formato: Fuente: Cursiva

Con formato: Disminuido 6 pto

Eliminado: T

Eliminado: E

Eliminado: also

Con formato: Fuente: Cursiva

Eliminado: Following the original neural nets analogy of Kohonen (1995), C_k is connected to each of the components of the data space through a weight vector v_k .

dictates how much intra cluster spread is represented by the classes. A broader range of patterns with more gradual differences is easily produced by increasing the number of clusters.

A clear advantage of SOM is the way the set of reference vectors, best representing different clusters within the data, is obtained. It uses an unsupervised learning process which minimizes an overall within-cluster distance from the data vectors, or patterns, x_i, to the corresponding reference vectors

$$\sum_{k=1...m}^{N} \sum_{x_i \in C_k} \left\| x_i - v_k \right\|^2 \qquad (9)$$

Eliminado: 3

where N is the number of available patterns (744 monthly patterns for the period 1948-2008). The aim of the training algorithm is iteratively adapting the reference vectors minimizing (9). First, the SOM clusters are initialized to random values. Then, the batch training proceeds in cycles: on each training cycle, a data sample x_i is considered and the best matching reference vector v_k is obtained as the one minimizing the Euclidean distance to the data vector:

Eliminado: 3

$$\left\| v_{w(i)} - x_i \right\| = \min_k \left\{ \left\| v_k - x_i \right\|, k = 1, ..., m \right\} \qquad (10)$$

Eliminado: 4

Then, the reference vector of the winning cluster is moved towards the sample vector based on a learning rate parameter in the algorithm. The learning rate controls how fast this process occurs, a small value leads to a slow and smooth learning process, while a high value produces a fast but unstable learning process (Gutierrez et al. 2005).

Eliminado: (

This training process includes a neighborhood adaptation mechanism so that neighboring clusters of the winning reference vector in the 2D matrix space are also adapted towards the sample vector. The number of adjacent clusters that are modified is specified by the radius of the training area, and the amount of adjustment varies: i) in inverse proportion to the distance from the initially identified cluster, and ii) in proportion to the learning rate parameter.

As a consequence of the neighborhood algorithm, during the iterative training the SOM behaves like a flexible lattice folding onto the cloud formed by the data in the original n dimensional space. Both the learning rate and the neighborhood algorithm radius decrease monotonically with time, softening the folding process (a linear decay to zero is usually chosen for these functions). For a detailed description of the process, the reader is referred to Oja and Kaski 1999.

4. RESULTS

First we have computed the extreme wave climate analysis in each location of the NE Atlantic. Figure 3 shows, for the six locations of interest, the seasonal and interannual modeling of the extreme wave height. Left panels show seasonality results. Note the variation throughout the year of the seasonal-dependant location and scale parameters and the seasonal-dependent quantile associated with the 50-year return period. The annual cycle is clear in all locations, particularly in Bretagne and Lisbon. The North Point shows a slightly asymmetric annual cycle, with higher events in autumn (October-November), which is accounted for throughout the shape parameter. Landes shows a long severe season that spans from October-November to March, but it presents milder extreme wave climate than North Point, Bretagne and Coruña, which is at similar latitude ($H_{50} \approx 10$ m in winter). Coruña, Lisbon and Azores present similar

Eliminado: cero

Eliminado: Note that we use the PC vectors u_i instead the original data x_i to train the SOM (Gutierrez et al. 2005).

Eliminado: ¶
3.3 Time-dependent extreme model¶
. Latest advances in extreme value theory (see Coles 2001) allow a better description of the natural climate variability of extreme events of geophysical variables, specifically extreme wave height. In this work a time-dependent GEV model for monthly maxima SWH including seasonal and interannual variability is used. We have considered time-dependent location $\mu(t)$, scale $\psi(t) > 0$ and shape $\xi(t)$ parameters of the GEV (Coles 2001), with cumulative distribution function (CDF) of Z_t (monthly maxima of the significant wave heights observed in month t) given by¶
¶

$$F_t(z) = \begin{cases} \exp\left\{-\left[1+\xi(t) \right.\right. \\ \exp\left\{-\exp\left[\right.\right. \end{cases}$$

, ... ¶
(5)¶
where $[a]_+ = \max[a, 0]$.
The GEV distribution includes the three classical distribution families of extreme value theory: Gumbel family ($\xi = 0$); Fréchet distribution ($\xi > 0$), and Weibull family ($\xi < 0$).¶
. Figure 2 shows the total population of SWH for each location and the monthly maxima sample. A clear seasonal variation is observed in all the points (stronger in north latitudes, North Point and Bretagne) and also a clear interannual variability can be appreciated, with severe and mild years, due to the natural climate variability. Since most of the variability is explained by seasonal behavior (Izaguirre et al. 2011) the introduction of harmonic functions to model seasonality is used (Menéndez et al., 2009). We let the model introduce the best number of harmonics in the three parameters.¶
. On the other hand, the ... [1]

extreme wave climate in terms of severity. However, Coruña shows a more complex parametrization due to the different sea families that arrive at this location in different parts of the year.

In the right panels, the interannual variability of the time-dependent 50-year return period quantile, δH_{50}, is presented. Note the variation of intensity between locations, reaching 4.8 m of significant wave height anomaly in the North Point, while only 1.2 m is reached in Azores. A variation in the intensity of the anomaly in every point is also observed. The northern points have more marked interannual variability whilst Coruña and Lisbon are less affected by the regional patterns of the North Atlantic having milder interannual variability.

Eliminado: ¶

SOMs have been applied for meteorological problems, for instance Cavazos (2000) classifying climate modes, Gutierrez et al. (2005) analyzing multi-model seasonal forecast, Cassano et al. (2006) classifying synoptic patterns in the western Artic or Reusch et al. (2007) classifying the North Atlantic climate variability. Depending on the purpose of the work, the lattice size of the SOM is different. After some preliminary tests, we have considered a SOM lattice of 8 x 8 = 64 groups, which fulfils the compromise between a significant number of weather types and the requirement of a minimum number of data per group.

Figure 4 shows the fields forming the atmospheric patterns for the resulting reference vectors of the 8 x 8 SOM, the weather types of the North Atlantic. In this figure one can see similar states close to each other and the most extreme states located at the corners. The most common well-known patterns can be identifying in the grid. The weather type located in the lower right corner corresponds to the synoptic situation of the positive phase of the NAO, characterized by low pressures centered in the south of Iceland and high pressures in the Azores Islands. The surrounding cells show transition states with variations of the synoptic pattern, till the negative phase, found approximately in the middle rows of the left columns. On the other hand, the upper left weather type shows a very different situation, characterized by positive anomaly of pressure centered above the north-western part of Europe, similar to a blocking situation describe by Cassou et al. (2011). The Atlantic Ridge weather regime describe in Cassou et al. (2011) can be found in the upper right corner, and the positive phase of the East Atlantic pattern (north-south dipole anomalies, similar to NAO but southerly shifted) in the middle maps of the last row.

Eliminado: the opposite

Eliminado: high pressures

Eliminado: in Great Britain

The distribution from the high-dimensional space can be transformed into probability density function on the SOM lattice. Each centroid, c_i, has a probability of occurrence, p_i (figure 5), according to the histogram of winner clusters for each atmospheric data, so that $\sum_{i=1}^{N} p_i = 1$, where N is the SOM size ($N = 64$ in this case). The extreme wave climate can be projected similarly, representing in each cell the average value of the corresponding MSLP dates within each cluster in order to establish the relationship between the atmospheric conditions and extreme wave climate.

In this section, we establish a connection between the study of atmospheric patterns in the North Atlantic and the extreme wave climate in different locations. Note that the SOM technique, besides obtaining the most representative synoptic situations in the NE Atlantic, also provides the possibility of representing a local climate variable at a particular location on the SOM lattice by projecting the variable value associated to each MSLP field. The process is summarized as follows:

1) We obtain synoptic atmospheric situations clustering standardized MSLP (in terms of PCs) by using SOM pattern (figure 3).

2) For a specific location, using the standardized MSLP dates, we identify the corresponding wave data of each cluster.

3) For each cluster we calculate the monthly quantile anomalies of extreme SWH (in terms of interannual variability) subtracting the seasonal-dependent quantile from the time-dependent quantile.

4) We calculate the mean quantile anomaly of extreme SWH in each cluster, together with its significance at 10 % level, and show the results in SOM-lattice format (figure 6).

Figure 6 shows the monthly extreme wave anomaly function on the SOM lattice for each location. Significant values at 10 % level are represented with a dot in the middle of the cell. One can see higher interannual variability in the northern points, reaching 2.5 m of positive anomaly in the North Point, while in Azores the higher interannual anomaly reaches 1 m. This graphical representation, together with the weather types, provide an easy way to identify atmospheric situations that produce positive or negative anomalies (interannual variability) in the extreme wave climate at a specific location. The anomaly in each cell is linked with its corresponding synoptic pattern. Note that smooth variations of the quantile anomalies through the SOM lattice and clear groups of SOM states generate an increase or decrease in the H_{50}. For instance, in the North Point the weather types located in the first columns, characterized by positive anomaly of pressure centred above Iceland and northern Great Britain generate negative anomalies in the extreme wave climate (up to -1.5 m). On the other hand, during years characterized by atmospheric situations located in the last columns of the lattice (positive phase of the NAO situation) the extreme wave climate in North Point increases (positive anomaly reaching 2.5 m). These results are consistent with those obtained in Wang and Swail (2002), where the winter seasonal 99th percentile of

Eliminado: U
Eliminado: in each cluster
Eliminado: for a specific location
Eliminado: 5
Eliminado: 5
Eliminado:
Eliminado: n
Eliminado: increament
Eliminado: decreament
Eliminado: high
Eliminado: s
Eliminado: e
Eliminado: in
Eliminado: and low pressures above the Iberian Peninsula,
Eliminado: around
Con formato: Superíndice

SWH in the North Atlantic is predicted by a NAO-like structure of SLP. Dodet et al. (2010) also showed high correlation between the NAO index and winter wave parameters, finding higher correlation at northern latitudes, north of 55º, where the North Point of this study is located. In the case of Bretagne, Landes and Coruña, the positive/negative extreme wave anomaly pattern in the SOM lattice is quite similar, varying slightly with respect to the intensity of the anomaly. The characteristic synoptic situation of positive phase of NAO (weather type in the lower right corner) generates positive anomalies of extreme wave height, especially in Bretagne and Landes (up to 2 m). Besides, the states in the last row, representing the East Atlantic pattern, generate lower intensity of positive extreme wave height anomalies. Note that the positive phase of NAO accounts for increased storminess in the mid North Atlantic but also de East Atlantic pattern is an important factor for the storminess in the middle of the North Atlantic (Seierstad et al., 2007). It is also remarkable the positive extreme wave height anomaly generate by the Atlantic Ridge (weather type in the upper right corner). On the other hand, the negative anomalies are generated by the blocking situation and transition states (upper left corner and surroundings). Lisbon shows negative anomalies of extreme wave height (≈ -0.8 m) related to weather types similar to a blocking situation, characterized by positive anomaly of pressure centred over the north-western part of Europe, and the dipole of anomalies in the east-west direction. Finally, Azores shows a different positive/negative wave extreme anomaly pattern in the SOM lattice. In this case, the weather types located in the last column and first row generate the higher negative anomalies (up to -1 m). The weather types in the last column can be related to the positive phase of the NAO pattern and transition states. The ones in the first row are more similar to a blocking situation. On the contrary, weather types characterized by

Eliminado: high

Eliminado: s located in the northeast of the North Atlantic basin. Most of them are transition states of the negative phase of the NAO situation.

Eliminado: s

Eliminado: around

Eliminado: se

Eliminado: correspond

negative anomaly of pressure over the central North Atlantic generate an increment in the extreme wave climate.

Eliminado: high

Eliminado: s

Eliminado: Islands

In conclusion, it is remarkable that this technique allows identifying the synoptic patterns responsible of an increase in the extreme wave height of a specific place. Note that those synoptic patterns depend on the location of the studied point.

6. CONCLUSIONS

A methodological framework based on the SOM technique which provides a simple graphical representation of the link between the interannual variability of extreme wave climate with the synoptic patterns in the North Atlantic is presented.

The SOM classification is applied to principal components of monthly MSLP anomalies to characterize a synoptic climatology of the North Atlantic area. The resulting map shows patterns with variability in the Azores High and in the Icelandic Low and smooth transitions between climate states.

On the other hand, a time-dependent GEV model including seasonal and interannual variability is used to model the extreme wave height in six reanalysis locations in the North Atlantic. Interannual variability is considered to depend on the PCs of the monthly MSLP anomalies of the NA (Izaguirre et al. 2010). The best model has been fitted to each reanalysis point. The annual cycle is observed in all locations, with Coruña, Landes and Azores presenting the more complex parametrizations.

The 50-year return-period quantile anomalies for the studied locations have been projected into the SOM lattice, obtaining maps that link the positive or negative anomaly with the correspondent synoptic pattern. The projection of the extreme wave climate allows comparing different severity between locations and identifying the most energetic extreme wave families due to different atmospheric situations. Results show

Eliminado: .

Eliminado: Concerning to the interannual variability we have obtained maps that link the positive or negative anomaly with the correspondent synoptic pattern.

more influence of the interannual variability in the northern located points, where synoptic patterns with a low pressure center near Iceland increase the 50-year return-period quantile in the North Point by almost 2.5 m.

Eliminado: in

The simplicity of evaluating the synoptic patterns using the SOM technique and the representation of the consistent anomalies of extreme wave height in a certain location on the synoptic SOM lattice, provide a useful and easy descriptive graphical representation that helps understanding the effect of synoptic patterns at a global scale on extreme wave climate at a regional scale.

Acknowledgements

C. Izaguirre is indebted to the Universidad de Cantabria and the Gobierno de Cantabria for the funding provided within the Posdoctoral Support Program. The work was partially funded by projects “GRACCIE” (CSD2007-00067, CONSOLIDER-INGENIO 2010) and “AMVAR” (CTM2010-15009) from the Spanish Ministry of Ciencia e Innovación, “MARUCA” from the Spanish Ministry of Fomento and “C3E” from the Spanish Ministry of Environment, Rural and Marine. We also want to thank the two anonymous reviewers for their useful comments that contributed to the final version of the manuscript.

REFERENCES

Ancell R., and J.M. Gutiérrez, 2008: High resolution probabilistic forecast using Bayesian networks. *EMS Annual Meeting 2008*. European Conference on Applied Climatology (ECAC).

Bacon and Carter, 1993: A connection between mean wave height and atmospheric pressure gradient in the North Atlantic. *Int. J. Climatol.*, **13**, 423-436.

Barry, R.G., and A.H. Perry, 1973: *Synoptic climatology: methods and applications.* Methuen & Co Ltd, London.

Bermejo M., and R. Ancell, 2009: Observed changes in extreme temperatures over Spain during1957-2002, using weather types. *Revista de Climatología*, **9**, 45-61.

Caires, S., V.R. Swail, and X.L. Wang, 2006: Projection and analysis of extreme wave climate. *J. Climate*, **19(21)**, 5581-5605.

Cassano, E.N., A.H. Lynch, J.J. Cassano, and M.R. Koslow, 2006: Classifiction of synoptic patterns in the western Artic associated with extreme events at Barrow, Alaska, USA. *Climate Research*, **30**, 83-97.

Cassou C, M. Minvielle, L. Terray, and C. Périgaud, 2011: A statistical-dynamical scheme for reconstructing ocean forcing in the Atlantic. Part 1: weather regimes as predictors for ocean surface variables, *Clim. Dyn*., **36**, 19-39.

Cavazos, T., 2000: Using Self-Organizing Maps to investigate extreme climate event: an application to wintertime precipitation in the Balkans. *J. Climate*, **13**,1718-1732.

Coles, S. G., 2001: *An introduction to statistical modelling of extreme values.* London: Springer, 208 pp.

Dodet, G., X. Bertin, and R. Taborda, 2010: Wave climate variability in the north-east Atlantic Ocean over the last six decades. *Ocean Modell*., **31**, 120-131.

Gutierrez J.M., R. Cano, A.S. Cofiño, and C.M. Sordo, 2004: Redes Probabilísticas y Neuronales en las Ciencias Atmosféricas, *Series Monográficas de AEMET*.

Con formato: Inglés (Reino Unido)

Con formato: Fuente: Cursiva

Con formato: Fuente: Negrita

Con formato: Inglés (Reino Unido)

Con formato: Fuente: Cursiva

Con formato: Fuente: Negrita

Con formato: Inglés (Reino Unido)

Gutiérrez, J.M., R. Cano, A.S. Cofiño, and C. Sordo, 2005: Analysis and downscaling multi-model seasonal forescast in Peru using Self-organizing Maps. *Tellus*, **57A**, 435-447.

Hemer, M.A., 2010. Historical trends in Southern Ocean storminess: Long-term variability of extreme wave heights at Cape Sorell, Tasmania. *Geophys. Res. Lett.*, **37**, L18601.

Izaguirre, C., F.J. Méndez, M. Menéndez, A. Luceño, and I.J. Losada, 2010: Extreme wave climate variability in Southern Europe using satellite data. *J. Geophys. Res*, **115**, C04009.

Izaguirre C., F.J. Méndez, M. Menéndez, and I.J. Losada, 2011: Global extreme wave height variability based on satellite data. *Geophys. Res. Lett.*, **38**, L10607.

Jolliffe, I.T., 2002: *Principal Component Analysis* (2nd ed). Springer, New York.

Kalnay, E., M. Kanamitsu, R. Kistler, W. Collins, D. Deaven, L. Gandin, M. Iredell, S. Saha, G. Walt, J. Woollen, Y. Zhu, M. Chelliah, W. Ebisuzaki, W. Higgins, J. Janowiak, K.C. Mo, C. Ropelewski, J. Wang, A. Leetmaa, R. Reynolds, R. Jenne, and D. Joseph, 1996: The NCEP/NCAR 40-year reanalysis project, *Bull. Amer. Meteor. Soc.,* **77**, 437–471.

Kohonen, T., 1995: *Self-Organizing Maps*. Number 30 in Springer Series in Information Sciences. Springer-Verlag.

Kohonen, T. 2001: *Self-Organizing Maps*. Springer-Verlag, Berlin, 3^{rd} ed.

Kushnir , Y., V.J. Cardone, J.G. Greenwood, and M.A. Cane, 1997: The recent increase in North Atlantic wave heights, *J. Climate*, **10**, 2107-2113.

Con formato: Fuente: Cursiva

Con formato: Fuente: Negrita

Le Cozannet, G., S. Lecacheux, E. Delvallee, N. Desramaut, C. Oliveros and R. Pedreros, 2011: Teleconnection Pattern Influence on Sea-Wave Climate in the Bay of Biscay. *J. Climate*, **24**, 641-652.

Méndez, F.J., M. Menéndez, A. Luceño, and I.J. Losada, 2006: Estimation of the long-term variability of extreme significant wave height using a time-dependent POT model. *J. Geophys. Res.*,**111**, C07024.

Menéndez, M., F.J. Méndez, C. Izaguirre, A. Luceño, and I.J. Losada, 2009: The influence of seasonality on estimating return values of significant wave height, *Coastal Eng.*, **56(3)**, 211-219.

Mínguez, R., F.J. Méndez, C. Izaguirre, M. Menéndez, and I.J. Losada, 2010: Pseudo-optimal parameter selection of non-stationary generalized extreme value models for environmental variables. *Env. Mod. & Software*, **25**, 1592-1607.

Mínguez, R., A. Espejo, A. Tomás, F.J. Méndez, and I.J. Losada, 2011: Directional Calibration of Wave Reanalisys Databases using Instrumental Data. *J. of Atmos. Oceanic Technol.* (in press). doi: 10.1175/JTECH-D-11-00008.1.

Oja, E., and S. Kaski, 1999: Kohonen maps. *Elsevier*, Amsterdam.

Preisendorfer, R.W., and C.D. Mobley, 1988: *Principal component analysis in meteorology and oceanography.* Developments in Atmospheric Science. Elsevier, Amsterdam.

Reguero, B.G., M. Menéndez, F.J. Méndez, R. Mínguez, and I.J. Losada, 2012: A global Ocean Wave (GOW) calibrated reanalysis from 1948 onwards. *Coastal Engineering*, **65**, 38-55. Doi:10.1016/j.coastaleng.2012.03.003.

Reusch, D.B., R.B. Alley, and B.C. Hewitson, 2007: North Atlantic climate variability from a self-organizing map perspective. *J. Geophys. Res.*, **112**, D02104.

Seierstad, I.A., D.B. Stephenson, and N.G. Kvamstø, 2007: How useful are teleconnection patterns for explaining variability in extratropical storminess? *Tellus*, **59A**, 170-181.

Con formato: Fuente: Cursiva

Con formato: Fuente: Negrita

Smith, T.M., R.W. Reynolds, R.E. Livezey, and D.C. Stokes, 1996: Reconstruction of historical sea surface temperatures using empirical orthogonal functions. *J. Climate*, **9(6)**, 1403-1420.

Tolman, H.L., 2010: *WAVEWATCH III (R) development best practices Ver. 0.1*. NOAA / NWS / NCEP / MMAB Technical Note 286, 19 pp.

Wang, X.L., and V.R. Swail, 2001: Changes of extreme wave height in northern Hemisphere oceans and related atmospheric circulation regimes. *J. Climate*, **14**, 2204-2221.

Wang, X.L, and V.R. Swail, 2002: Trends of Atlantic wave extremes as simulated in a 40-yr wave hindcast using kinematically reanalyzed wind fields, *J. Climate*, **15**, 1020-1035.

Woolf, D. K., P. G. Challenor, and P. D. Cotton, 2002: Variability and predictability of the North Atlantic wave climate, *J. Geophys. Res*., **107(C10)**, 3145.

Con formato: Fuente: Cursiva

Con formato: Fuente: Negrita

Con formato: Inglés (Reino Unido)

FIGURE CAPTIONS

Figure 1. Spatial domain of the North Atlantic area and wave locations (NP, BR, LA, CO, LI and AZ stands for North Point, Bretagne, Landes, Coruña, Lisbon and Azores, respectively).

Figure 2. Time series of SWH (grey color) and monthly maxima (black line) for the six analyzed locations.

Figure 3. Left panels: maximum SWH data (grey dots), location (grey line) and scale (dashed grey line) parameters and 50-year return period quantile (black line). Right panels: time series of the anomalies of the time-dependent 50-year return period quantile (interannual variability).

Figure 4. Atmospheric synoptic patterns (using PCs of standardized MSLP derived from NCEP-NCAR data between 1948-2008) in a SOM lattice of a 8 x 8.

Figure 5. Probability of occurrence of each weather type.

Figure 6. Quantile anomalies (cm) associated to the 50-year return period projected in the SOM lattice for the six reanalysis points. Significant values at the 90 % confidence interval are dotted.

Eliminado: 5

Eliminado: points.

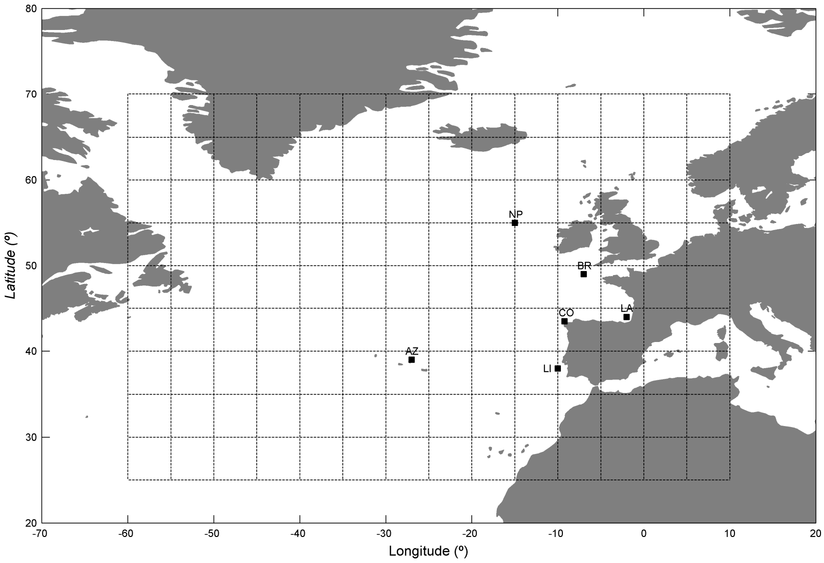

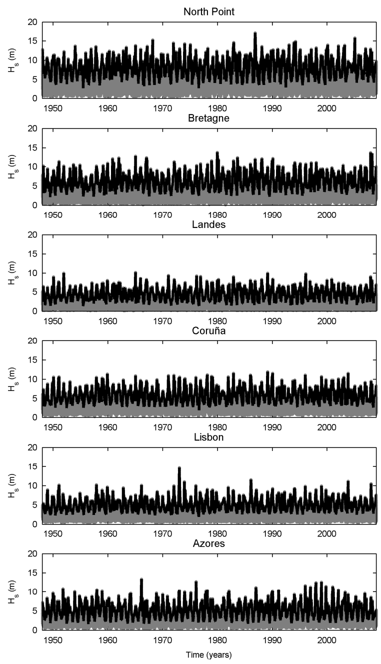
North Point
Bretagne
Landes
Coruña
Lisbon
Azores
H_s (m)
Time (years)

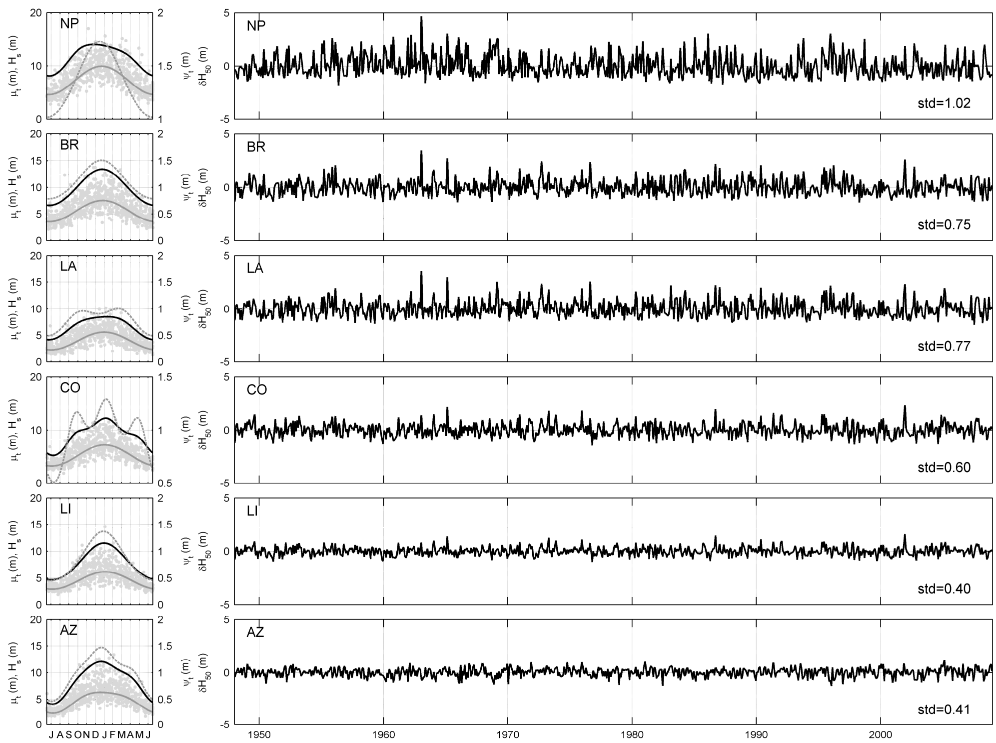
NP
BR
LA
CO
LI
AZ
μ_t (m), H_s (m)
ψ_t (m)
δH_{50} (m)
std=1.02
std=0.75
std=0.77
std=0.60
std=0.40
std=0.41
J A S O N D J F M A M J

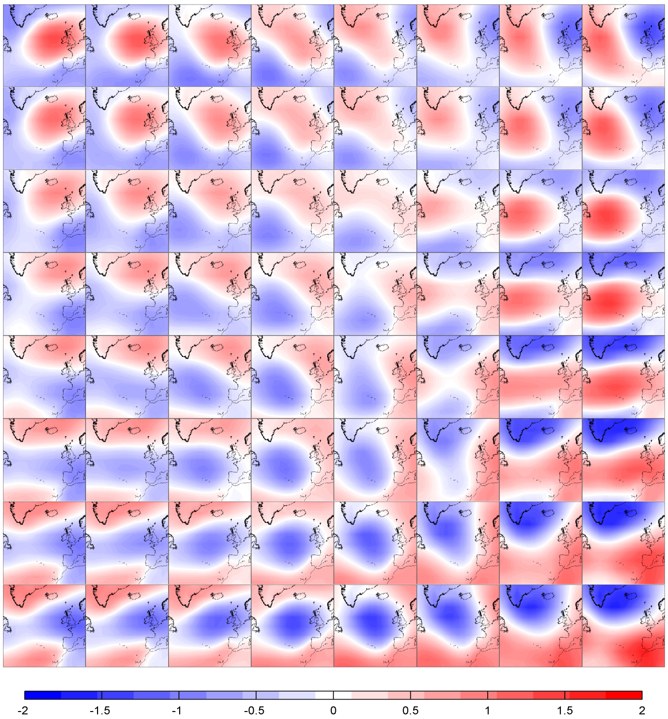
-2
-1.5
-1
-0.5
0
0.5
1
1.5
2

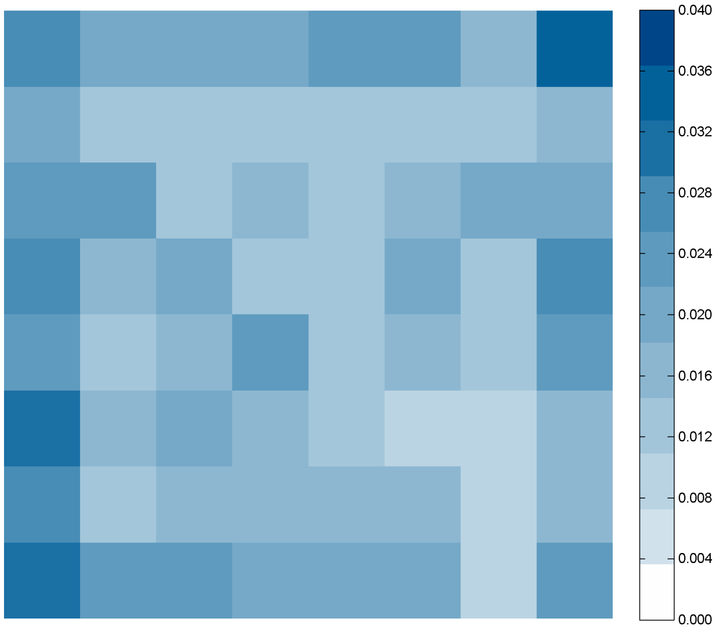
0.040
0.036
0.032
0.028
0.024
0.020
0.016
0.012
0.008
0.004
0.000

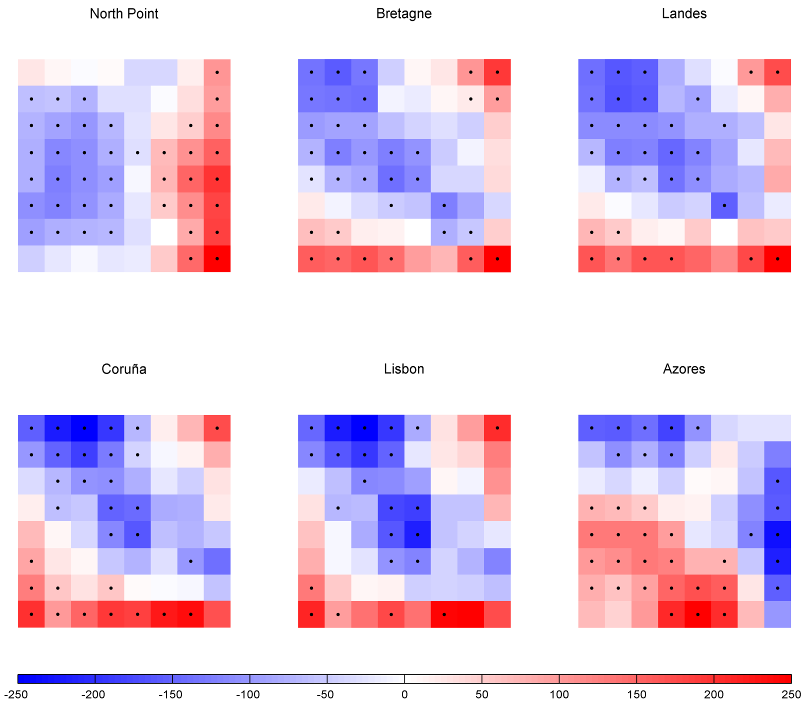
North Point
Bretagne
Landes
Coruña
Lisbon
Azores
-250
-200
-150
-100
-50
0
50
100
150
200
250

3.3 Time-dependent extreme model

Latest advances in extreme value theory (see Coles 2001) allow a better description of the natural climate variability of extreme events of geophysical variables, specifically extreme wave height. In this work a time-dependent GEV model for monthly maxima SWH including seasonal and interannual variability is used. We have considered time-dependent location $\mu(t)$, scale $\psi(t) > 0$ and shape $\xi(t)$ parameters of the GEV (Coles 2001), with cumulative distribution function (CDF) of Z_t (monthly maxima of the significant wave heights observed in month t) given by

$$F_t(z) = \begin{cases} \exp\left\{-\left[1+\xi(t)\left(\dfrac{z-\mu(t)}{\psi(t)}\right)\right]_+^{-1/\xi(t)}\right\} & \xi(t) \neq 0 \\ \exp\left\{-\exp\left[-\left(\dfrac{z-\mu(t)}{\psi(t)}\right)\right]\right\} & \xi(t) = 0 \end{cases}, \tag{5}$$

where $[a]_+ = \max\left[a, 0\right]$. The GEV distribution includes the three classical distribution families of extreme value theory: Gumbel family ($\xi = 0$); Fréchet distribution ($\xi > 0$), and Weibull family ($\xi < 0$).

Figure 2 shows the total population of SWH for each location and the monthly maxima sample. A clear seasonal variation is observed in all the points (stronger in north latitudes, North Point and Bretagne) and also a clear interannual variability can be appreciated, with severe and mild years, due to the natural climate variability. Since most of the variability is explained by seasonal behavior (Izaguirre et al. 2011) the introduction of harmonic functions to model seasonality is used (Menéndez et al., 2009). We let the model introduce the best number of harmonics in the three parameters.

On the other hand, the hypothesis that extreme wave climate is affected by regional SLP patterns is used and standardized PCs of monthly MSLP in the NE Atlantic are introduced as covariates to model interannual variability (Izaguirre et al., 2010). We let the model introduce up to ten PCs as linear terms in the location and scale parameter.

Mathematically, the model can be expressed as:

$$\mu(t)=\beta_0+\sum_{i=1}^{P_\mu}\left[\beta_{2i-1}\cos(i\omega t)+\beta_{2i}\sin(i\omega t)\right]+\sum_{j=1}^{10}\beta_{PCj}PC_j(t) \tag{6}$$

$$\log\left[\psi(t)\right]=\alpha_0+\sum_{i=1}^{P_\psi}\left[\alpha_{2i-1}\cos(i\omega t)+\alpha_{2i}\sin(i\omega t)\right]+\sum_{j=1}^{10}\alpha_{PCj}PC_j(t) \tag{7}$$

$$\xi(t)=\gamma_0+\sum_{i=1}^{P_\xi}\left[\gamma_{2i-1}\cos(i\omega t)+\gamma_{2i}\sin(i\omega t)\right] \tag{8}$$

where β_0, α_0 and γ_0 are mean values; β_i, α_i and γ_i ($i > 0$) are the amplitudes of the harmonics; $\omega = 2\pi$ year^{-1}; P_μ, P_ψ, and P_ξ determine the number of sinusoidal harmonics in a year; and t is given in years. The parameter β_{PCj} and α_{PCj} represents the influence on the location and scale parameters per unit of standardized PC_j in a particular month, t. The model selection is carried out using the pseudo-optimal method explained in Minguez et al. (2010).

The instantaneous quantile $z_q(t)$ associated with the return period $1/q$ can be obtained using:

$$z_q\left(\mu(t),\psi(t),\xi(t)\right)=\begin{cases}\mu(t)-\dfrac{\psi(t)}{\xi(t)}\left[1-\left\{-\log\left(1-q\right)\right\}^{-\xi(t)}\right] & \xi(\mathrm{t})\neq 0\\ \mu(t)-\psi(t)\log\left\{-\log\left(1-q\right)\right\} & \xi(\mathrm{t})=0\end{cases}$$

(9)

where probability q is given by $F_t(z)=1-q$. Since seasonal and interannual variability have been modeled, the quantile varies depending on the time within the year and the year itself.

The interannual variation in the time-dependent quantile can be expressed as the difference between the time-dependent quantile (z_q) and the seasonal-dependent quantile (z_{qs}), where the seasonal-dependent quantile is calculated from a regression model where only the seasonal variation is considered.

$$\delta z_q = z_q - z_{qs}$$

(10)

where δz_q is the time-dependent quantile anomaly.